



Aalborg Universitet

**AALBORG UNIVERSITY**  
DENMARK

## **Damping Inter-area Oscillations using Static Synchronous Series Compensator (SSSC)**

Su, Chi; Chen, Zhe

*Published in:*

Proceedings of the 46th IEEE International Universities' Power Engineering Conference (UPEC 2011)

*Publication date:*  
2011

*Document Version*  
Early version, also known as pre-print

[Link to publication from Aalborg University](#)

*Citation for published version (APA):*

Su, C., & Chen, Z. (2011). Damping Inter-area Oscillations using Static Synchronous Series Compensator (SSSC). In *Proceedings of the 46th IEEE International Universities' Power Engineering Conference (UPEC 2011)* (pp. 1-6). IEEE Press.

### **General rights**

Copyright and moral rights for the publications made accessible in the public portal are retained by the authors and/or other copyright owners and it is a condition of accessing publications that users recognise and abide by the legal requirements associated with these rights.

- Users may download and print one copy of any publication from the public portal for the purpose of private study or research.
- You may not further distribute the material or use it for any profit-making activity or commercial gain
- You may freely distribute the URL identifying the publication in the public portal -

### **Take down policy**

If you believe that this document breaches copyright please contact us at [vbn@aub.aau.dk](mailto:vbn@aub.aau.dk) providing details, and we will remove access to the work immediately and investigate your claim.

# Damping Inter-Area Oscillations Using Static Synchronous Series Compensator (SSSC)

Chi Su, Zhe Chen

Department of Energy Technology  
Aalborg University, Denmark  
csu@iet.aau.dk, zch@iet.aau.dk

**Abstract**—Static synchronous series compensator (SSSC) has the ability to emulate a reactance in series with the connected transmission line. When fed with some supplementary signals from the connected system, SSSC is able to participate in the power system inter-area oscillation damping by changing the compensated reactance. This paper analyses the influence of SSSC on power system small signal stability. A SSSC damping controller scheme is presented and discussed. In DIgSILENT PowerFactory software, modal analysis and time-domain simulation are conducted in a single-machine infinite bus system model and a four-machine two-area test system model to verify and improve the damping controller scheme.

**Index Terms**—small signal stability, static synchronous series compensator (SSSC), inter-area oscillation

## I. INTRODUCTION

Power system small signal stability is the ability of the power system to maintain synchronism among generators under small disturbances. In the early age of power system, small signal instability problem used to appear as oscillations among generator rotors within the same plant and this was solved by amortisseurs implemented in generator rotors. Later with the application of fast excitation system, there appeared electromagnetic oscillations in high-loaded power systems, while this was solved by the development and utilization of Power System Stabilizers (PSS). However, in modern power systems, due to the connection of power grids in vast areas, a type of low-frequency oscillation appeared among different areas, namely, inter-area oscillation mode. For inter-area oscillation damping, conventional PSS based on local input signal is not effective enough. In this situation, adaptive and robust methods are in need for PSS design, while due to the ability of controlling line impedance, power flow and bus voltage, Flexible AC Transmission System (FACTS) device implementation offers an alternative solution [1].

Static Synchronous Series Compensator (SSSC) is based on voltage source convertor. It is connected in series with a transmission line and injects an almost sinusoidal voltage which is nearly in quadrature with the line current. In this way SSSC can emulate a reactance in series with the transmission line and it could be inductive if the injected voltage is leading the line current and capacitive the other way. When feeding some supplementary signals to the SSSC

controller, the SSSC may participate in the oscillation damping by changing the compensated reactance.

The authors of [2] investigated the application of series compensator in damping power system oscillation on the basis of the Phillips-Heffron model, with the assumption that the compensator is ideal. With a linearized model of SSSC, a damping controller with the scheme of a traditional power system stabilizer (PSS) is studied in [3]. Two voltage regulator schemes in SSSC are compared in [4] and the same authors further investigated a power system oscillation damping controller scheme in SSSC in [5]. With same damping controller scheme in [5], the author of [6] uses the transmission line power deviation as the input instead of the generator speed deviation and studies the performance of the damping controller in a power system with large wind farm. In [7], the author develops a damping controller for SSSC based on adaptive neuro-control.

This paper investigates the influence of SSSC on power system small signal stability and presents the SSSC damping controller scheme. Modal analysis and time domain simulation on a single-machine infinite bus system and a four-machine two-area test system is conducted in the software DIgSILENT PowerFactory.

The rest of the paper is organized as follows: brief introductions to small signal stability and SSSC basic control strategies are respectively presented in section II and section III. The influence of SSSC on power system small signal stability is investigated in section IV and an SSSC damping controller is presented in section V. Case study is demonstrated in section VI while conclusions and future work are described in section VII.

## II. SMALL SIGNAL STABILITY

Small signal stability is the ability of a power system to maintain synchronism among generators under small disturbances.

A power system can be described by a state equation in the form of (1) (with the assumption of zero input).

$$\frac{dX}{dt} = f(X) \quad (1)$$

In (1),  $X$  denotes the state vector of the power system,  $t$  denotes the time and  $f$  is normally a set of nonlinear functions.

To analyze the small signal stability of the power system at an operating point, the first step is to linearize the state equation at this operating point by Taylor's series expansion. The linearized state equation is in the form of (2).

$$\frac{d\Delta X}{dt} = A \cdot \Delta X \quad (2)$$

In (2), the prefix  $\Delta$  denotes a small deviation and  $A$  is the state matrix. The small signal stability is given by the eigenvalues of matrix  $A$ . Eigenvalues are in the form of (3).

$$\lambda = \sigma \pm j \cdot \omega \quad (3)$$

Each eigenvalue (or a conjugate pair) corresponds to an oscillation mode of the power system at the analyzed operating point. The real component of the eigenvalues  $\sigma$  gives the damping and the imaginary component  $\omega$  gives the frequency of the corresponding mode. The small signal stability is then determined as follows:

- when all eigenvalues have negative real parts, the system is stable;
- when at least one eigenvalue has positive real part, the system is unstable;
- when at least one eigenvalue has zero real part, the stability of the system can not be told in this way.

The information of the decay rate of the oscillation can be also drawn from eigenvalues by a calculating variable termed as damping ratio which is in the form of (4).

$$\zeta = \frac{-\sigma}{\sqrt{\sigma^2 + \omega^2}} \quad (4)$$

This is a common index of small signal stability analysis. The larger  $\zeta$  is, the system is considered to have wider stability margin.

To measure the participation of one state variable in one oscillation mode, we use participation factor in the form of (5).

$$p_{ik} = \frac{\partial \lambda_i}{\partial a_{kk}} \quad (5)$$

In (5),  $p_{ik}$  denotes the participation factor of the  $k$ th state variable in the  $i$ th mode and  $a_{kk}$  denotes the element in the  $k$ th line and  $k$ th column of matrix  $A$  [8][9].

### III. SSSC AND ITS VOLTAGE REGULATOR

Fig.1 shows an SSSC connected in a single-machine infinite bus system. Voltage  $V_c$  generated from SSSC could be controlled by Pulse Width Modulation (PWM) method in such a way that it is always kept in quadrature with  $I_t$  and

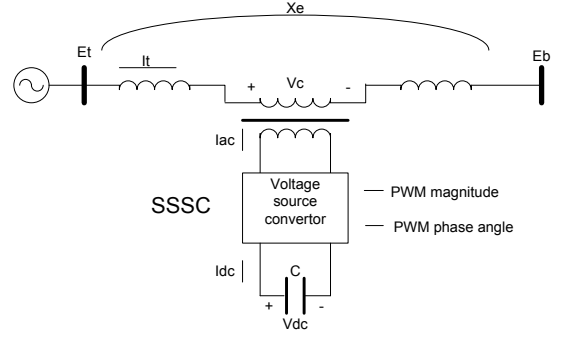


Fig.1. SSSC connected in a single-machine infinite bus system

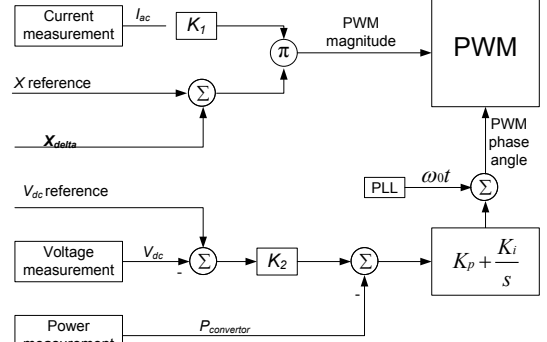


Fig.2. SSSC voltage regulator scheme

Therefore, SSSC appears as a compensated capacitance or inductance in the connected system. The PWM magnitude controls the volume of this compensated reactance and the PWM phase angle decides whether it is capacitive or inductive [4][10].

The voltage regulator scheme which produces the PWM magnitude and PWM phase angle signals is depicted in Fig.2 [4]. PWM magnitude signal is obtained by multiplying the AC current measurement  $I_{ac}$  in SSSC and the reactance reference value  $X_{delta}$  in Fig.2 is from an external damping controller which will be discussed in section V. PWM phase angle signal is produced by adding a PI controller output to a synchronous phase angle. This PI controller is used to keep the DC voltage  $V_{dc}$  constant so that there is no active power input to or output from SSSC, therefore, the result PWM phase angle makes sure that  $V_c$  is in quadrature with  $I_t$  and SSSC appears as a reactance.

### IV. INFLUENCE OF SSSC ON SMALL SIGNAL STABILITY

The single-machine infinite bus system in fig.1 is considered. In small signal stability analysis, the stator dynamics of the synchronous generator can be ignored [8]. For mathematical simplicity, all amortisseur circuits in synchronous generator rotor and all resistance are ignored. As a result, there is only one electric differential equation left which is the field circuit voltage equation. Plus two differential equations of synchronous generator motion, the third-order state equation of the single-machine infinite bus system is presented as (6).

$$\begin{aligned}
p\omega_r &= \frac{1}{2H}(T_m - T_e - K_D\omega_r) \\
p\delta &= \omega_0\omega_r \\
p\Psi_{fd} &= \frac{\omega_0 R_{fd}}{L_{adu}} E_{fd} - \omega_0 R_{fd} i_{fd}
\end{aligned}
\tag{6}$$

In (6),  $p$  is the differential operator;  $\Delta\omega_r$  is the generator rotor speed deviation;  $H$  is the generator per unit inertia constant;  $T_m$  is the mechanical torque,  $T_e$  is the electromagnetic torque;  $K_D$  is the mechanical damping coefficient;  $\delta$  is the generator rotor angle;  $\omega_0$  is the nominal generator speed;  $\Psi_{fd}$  is the field circuit flux linkage;  $R_{fd}$  is the field circuit resistor;  $E_{fd}$  is the exciter output voltage;  $L_{adu}$  is the unsaturated value of mutual inductance between rotor and stator in d-axis;  $i_{fd}$  is the field circuit current [8].

In order to express the complete form of the state equation, it is needed to express  $T_e$  and  $i_{fd}$  in terms of the state variables which can be obtained from machine flux linkage equations, machine voltage equations and network equations as (7)-(11).

The electromagnetic torque equation:

$$T_e = \Psi_{ad} i_q - \Psi_{aq} i_d \tag{7}$$

where  $\Psi_{ad}$  and  $\Psi_{aq}$  are the d-axis and q-axis component of the generator mutual flux linkage between stator and rotor;  $i_d$  and  $i_q$  are stator currents.

Field circuit flux linkage equation:

$$i_{fd} = \frac{\Psi_{fd} - \Psi_{ad}}{L_{fd}} \tag{8}$$

where  $L_{fd}$  is the field circuit self inductance.

Mutual flux linkage equations:

$$\begin{aligned}
\Psi_{ad} &= -L_{ads} i_d + L_{ads} i_{fd} \\
\Psi_{aq} &= -L_{aqs} i_q
\end{aligned}
\tag{9}$$

where  $L_{adu}$  is the saturated value of mutual inductance between rotor and stator in d-axis.

Stator voltage equations:

$$\begin{aligned}
e_d &= L_l i_q - \Psi_{aq} \\
e_q &= -L_l i_d + \Psi_{ad}
\end{aligned}
\tag{10}$$

where  $e_d$  and  $e_q$  are the d-axis and q-axis component of the generator terminal voltage ( $E_t = e_q + j e_d$ ) and  $L_l$  is the leakage inductance in the stator circuit.

Network equations:

$$\begin{aligned}
e_d &= -X_E i_q + e_{bd} \\
e_q &= X_E i_d + e_{bq}
\end{aligned}
\tag{11}$$

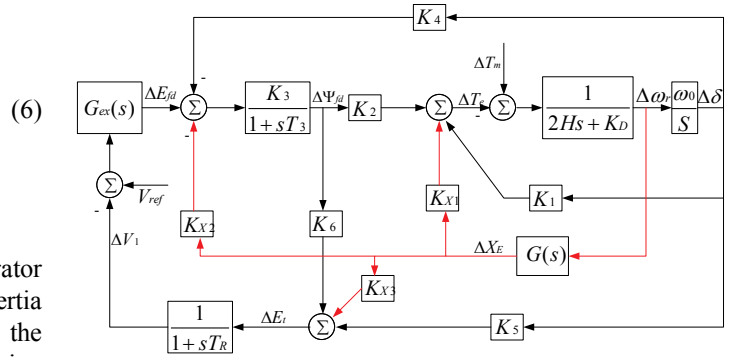


Fig.3. Block diagram representation of system

where  $X_E$  is the equivalent transmission line reactance as shown in fig.1.; while  $e_{bd}$  and  $e_{bq}$  are the d-axis and q-axis component of the infinite bus voltage  $E_b$  in fig.1.

For small signal analysis, it is required that the state equations are linearized, thus (7)-(11) should be expressed in terms of perturbed values. A little different from [8], because it is of interest to analyze the influence of SSSC on small signal stability, a term of  $\Delta X_E$  which is the transmission line reactance deviation is obtained in linearization of the equations. After solving equations (10) and (11), rearranging equations (7), (8) and (9), and substituting into state equation (6), a block diagram representation of the small signal performance of the single-machine infinite bus system is obtained as shown in Fig.3.

In Fig.3,  $G_{ex}(s)$  is the transfer function of the exciter and  $G(s)$  is the transfer function of the SSSC damping controller.  $K_1, K_2, K_3, K_4, K_5$  and  $K_6$  are the so-called K constants whose expressions can be found in [8]. Assuming that the SSSC can respond to  $X_{delta}$  in Fig.2 with no delay,  $\Delta X_E$  equals to  $X_{delta}$ . The red paths in the block diagram demonstrate the influence introduced by SSSC damping controller. The expression of  $K_{X1}, K_{X2}$  and  $K_{X3}$  are shown in (12).

$$\begin{aligned}
K_{X1} &= (n_3 + n_4)(\Psi_{ad0} + i_{d0} L_{aqs}) - (m_3 + m_4)(i_{q0} L'_{ads} + \Psi_{aq0}) \\
K_{X2} &= \frac{L_{adu} L'_{ads}}{L_{fd}} (m_3 + m_4)
\end{aligned}
\tag{12}$$

$$K_{X3} = \frac{e_{d0}}{E_{t0}} (L_l + L_{aqs})(n_3 + n_4) - \frac{e_{q0}}{E_{t0}} (L_l + L'_{ads})(m_3 + m_4)$$

where  $m_3, m_4, n_3$  and  $n_4$  are presented in (13).

$$\begin{aligned}
m_3 &= \frac{\Psi_{fd0} \frac{L_{ads}}{L_{ads} + L_{fd}} - e_{bq0}}{D} \\
m_4 &= \frac{-(L_l + X_{E0} + L_{aqs})(2X_{E0} + L_{aqs} + L'_{ads})m_3}{D} \\
n_3 &= \frac{e_{bd0}}{D} \\
n_4 &= -\frac{(L_l + X_{E0} + L_{aqs})(2X_{E0} + L_{aqs} + L'_{ads})n_3}{D}
\end{aligned}
\tag{13}$$

The expressions of  $L'_{ads}$  and  $D$  can be found in [8].

The contribution of SSSC damping controller to the electromagnetic torque is through blocks  $K_{X1}$ ,  $K_{X2}$  and  $K_{X3}$ . It can also be observed from Fig.3 that only the contribution through  $K_{X1}$  is direct, while the contribution through  $K_{X2}$  and  $K_{X3}$  is attenuated by first-order lag components. According to [2],  $K_{X2}$  and  $K_{X3}$  are neglectable compared with  $K_{X1}$ . When designing SSSC damping controller, in order to contribute to the electromagnetic torque a damping component which is in phase with  $\Delta\omega_r$ ,  $G(s)$  should offer 0 or 180 deg phase shift depending on if  $K_{X1}$  is positive or negative.

However, for multi-machine systems, (6)-(11) become matrix equations, while  $K_1$ ,  $K_2$ ,  $K_3$ ,  $K_4$ ,  $K_5$ ,  $K_6$ ,  $K_{X1}$ ,  $K_{X2}$  and  $K_{X3}$  all become matrices or vectors relating corresponding variables among different machines. The block diagram in Fig.3 still applies, but with each block as a matrix or a vector, the variables within different generators are coupled.

## V. SSSC DAMPING CONTROLLER

The SSSC damping controller scheme is shown in Fig.4.

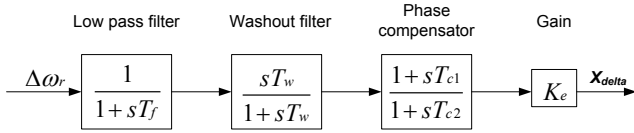


Fig.4. SSSC damping controller scheme

The low pass filter is adopted to filter high frequency variance in the input speed deviation. The frequency range of interest for small signal stability problem is 0.1Hz to 2.0Hz and the cutoff frequency of this filter is selected as 10Hz.

The washout filter works as a high pass filter which allows signals associated with oscillations in  $\Delta\omega_r$  to pass unchanged, whereas the steady change in  $\Delta\omega_r$  will be filtered.

Therefore these two filters mentioned above make sure that the damping controller only responds to signals in the form of oscillations within the frequency range of interest in small signal stability problem.

The phase compensator component provides an appropriate phase characteristics to compensate the phase shift introduced by the above mentioned filters so as to make the output  $X_{delta}$  from the damping controller be in phase with the input  $\Delta\omega_r$ . This compensation should cover the frequency range of interest and in multi-machine cases it is possible that the required total phase shift of the damping controller is some value other than zero.

## VI. CASE STUDY

### A. Single-machine infinite bus system

A single-machine infinite bus system with an SSSC connected in the transmission line as that in Fig.1 is built in DIgSILENT PowerFactory. The synchronous generator is

TABLE I  
DAMPING CONTROLLER PARAMETERS IN SINGLE-MACHINE INFINITE BUS SYSTEM

Parameters	$T_f$	$T_w$	$T_{c1}$	$T_{c2}$	$K_e$	Total phase shift of the damping controller
CASE1	0.0165	2.8	0.05	0.075	10	0
CASE2	0.0165	2.8	0.075	0.45	16	-36 deg

TABLE II  
OSCILLATION MODE IN SINGLE-MACHINE INFINITE BUS SYSTEM

Single-machine system	Oscillation mode frequency	Oscillation mode damping ratio
Without damping	0.447Hz	12.40%
CASE1	0.447Hz	24.90%
CASE2	0.485Hz	18.60%

simulated as a sixth-order model and the convertor in the SSSC is simulated as an average model. An SSSC damping controller designed according to the previous section is implemented in the simulation. Two sets of parameters of the damping controller are shown in TABLE I.

Using the modal analysis function of DIgSILENT PowerFactory, the complete information about all the eigenvalues of the system can be obtained. For the target single-machine infinite bus system, there is only one conjugate pair eigenvalue related to electromechanical oscillation. The frequency of this oscillation mode is around 0.45Hz. At this frequency, the total gain of the damping controller for the two sets of parameters are kept the same, while the total phase shifts of the damping controller for the two sets of parameters are shown in TABLE I. The oscillation mode frequency and damping ratio under three different damping conditions are shown in TABLE II. When there is no damping controller in SSSC, the oscillation damping ratio is 12.40%. When a damping controller with 0 phase shift is implemented, the damping ratio is increased to 24.90%. When a damping controller with -36 deg phase shift is implemented, the damping ratio is also increased, but with a lower level, to 18.60%. These results support the conclusions in section IV for single machine infinite bus system.

To validate the modal analysis results, time domain simulations with a three phase event at 5s are conducted under the three conditions and the active power generation from the synchronous generator is shown in Fig. 5

### B. Four-machine two-area test system

A four-machine two-area test system with a connected SSSC as shown in Fig.6 is built in DIgSILENT PowerFactory to study the multi-machine situation. Similar to the single-machine infinite bus model, the four synchronous generators in the four-machine system are also simulated as sixth-order model and the convertor in the SSSC is simulated as an average model.

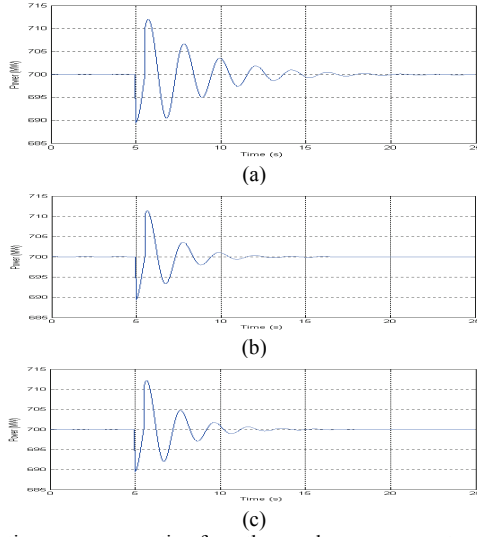


Fig.5. Active power generation from the synchronous generator of the single machine infinite bus system under different damping conditions: (a) no damping controller; (b) parameter CASE1; (c) parameter CASE2

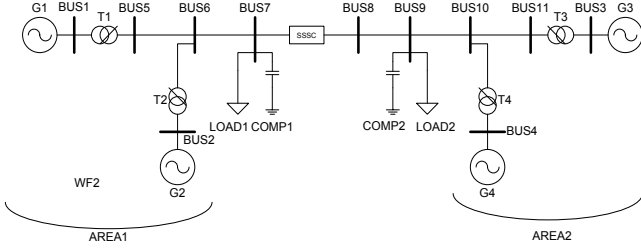


Fig.6. Four-machine two-area test system

Through modal analysis, three electromechanical oscillation modes are observed in this four-machine system, namely, an oscillation mode in area 1 (around 1.06Hz), an oscillation mode in area 2 (around 1.09Hz) and an oscillation between area 1 and area 2 (around 0.53Hz). Since the SSSC is located on the transmission line between area 1 and area 2, the inter-area oscillation mode is selected to design the SSSC damping controller. With regard to this inter-area mode, the participation factors, observability magnitudes and angles of the synchronous generator speed deviations are obtained from modal analysis and shown in TABLE III. It can be found in TABLE III that generators 3 and 4 in area 2 has the larger participation factors and observability magnitudes, while generators 1 and 2 in the other area have very small participation factors and observability magnitudes. Also it can be found that the generator speed deviations in area 1 are around 90 deg behind that in area 2 in the inter-area oscillation mode.

Considering the analysis in section IV,  $K_{Xl}$  is a four-element vector for this four-machine system, as depicted in (14).  $\Delta\omega_{ri}$  can be selected among the four generators. With the zero-phase-shift design of  $G(s)$  mentioned in section V,  $\Delta X_E$  is in phase with  $\Delta\omega_{ri}$ , and therefore,  $\Delta T_e$  in all four generators are in phase with  $\Delta\omega_{ri}$ . However, this is not necessarily the required situation.

TABLE III  
PARTICIPATION FACTORS AND OBSERVABILITY IN THE INTER-AREA OSCILLATION MODE

	Participation factors (relative to the largest one)	Observability magnitude (relative to the largest one)	Observability angle (relative to the largest one)
$\Delta\omega_{r1}$	0.0994	0.0952	257.407 deg
$\Delta\omega_{r2}$	0.0722	0.0933	287.461 deg
$\Delta\omega_{r3}$	1.0	1.0	0
$\Delta\omega_{r4}$	0.7262	0.8898	0.73 deg

TABLE IV  
DAMPING CONTROLLER PARAMETERS IN FOUR-MACHINE TWO-AREA SYSTEM

Parameters	$T_f$	$T_w$	$T_{c1}$	$T_{c2}$	$K_e$	Total phase shift of the damping controller
PARA1	0.0165	2.8	0.05	0.067	10	0
PARA2	0.0165	2.8	-1.2	0.075	-2.5	90 deg

TABLE V  
OSCILLATION MODE IN FOUR-MACHINE TWO-AREA SYSTEM

With or without damping controller	Input signal	Damping controller parameters	Oscillation mode frequency	Oscillation mode damping ratio
without	/	/	0.530Hz	4.10%
with	$\Delta\omega_{r3}$	PARA1	0.533Hz	10.96%
with	$\Delta\omega_{r1}$	PARA1	0.533Hz	3.85%
with	$\Delta\omega_{r1}$	PARA2	0.530Hz	4.79%

$$\begin{bmatrix} \Delta T_{e1} \\ \Delta T_{e2} \\ \Delta T_{e3} \\ \Delta T_{e4} \end{bmatrix} = \begin{bmatrix} K_{X11} \\ K_{X12} \\ K_{X13} \\ K_{X14} \end{bmatrix} \Delta X_E \quad (14)$$

$$\Delta X_E = G(s) \Delta\omega_{ri}$$

In the four-machine system, if we select  $\Delta\omega_{r3}$  as the input to the damping controller, then  $\Delta T_e$  in all four generators are in phase with  $\Delta\omega_{r3}$ , including  $\Delta T_{e1}$  and  $\Delta T_{e2}$  that are supposed to be respectively in phase with the 90-deg-behind  $\Delta\omega_{r1}$  and  $\Delta\omega_{r2}$ . But because generator 3 and generator 4 have much larger participation factors, once they respond to the oscillation in the right direction, good damping performance can be expected.

On the other hand, if we select  $\Delta\omega_{r1}$  as the input,  $\Delta T_e$  in all four generators will change in phase with  $\Delta\omega_{r1}$  at a much smaller level compared with the previous case due to the much smaller observability magnitude of  $\Delta\omega_{r1}$  than  $\Delta\omega_{r3}$ . But still, the more participating generators 3 and 4 would not change their electromagnetic torque in phase with their own speed deviation and this might cause some unexpected results.

In order to make the more participating generators 3 and 4 always change their electromagnetic torque in phase with their own speed deviation,  $G(s)$  could be designed as a 90-deg-lead

component when  $\Delta\omega_{r1}$  or  $\Delta\omega_{r2}$  is selected as input. Two sets of damping controller parameters designed at the inter-area oscillation mode frequency are interpreted in TABLE IV.

The inter-area oscillation frequency and damping ratio under four different damping controller conditions are shown in TABLE V.

As expected, when  $\Delta\omega_{r3}$  is the input, the zero-phase-shift design of the damping controller works with a broad increase in damping ratio compared with the case without damping controller. While when  $\Delta\omega_{r1}$  is the input, the zero-phase-shift design of the damping controller even introduces a decrease in the damping ratio. This situation could be changed using the 90-deg-lead design of the damping controller.

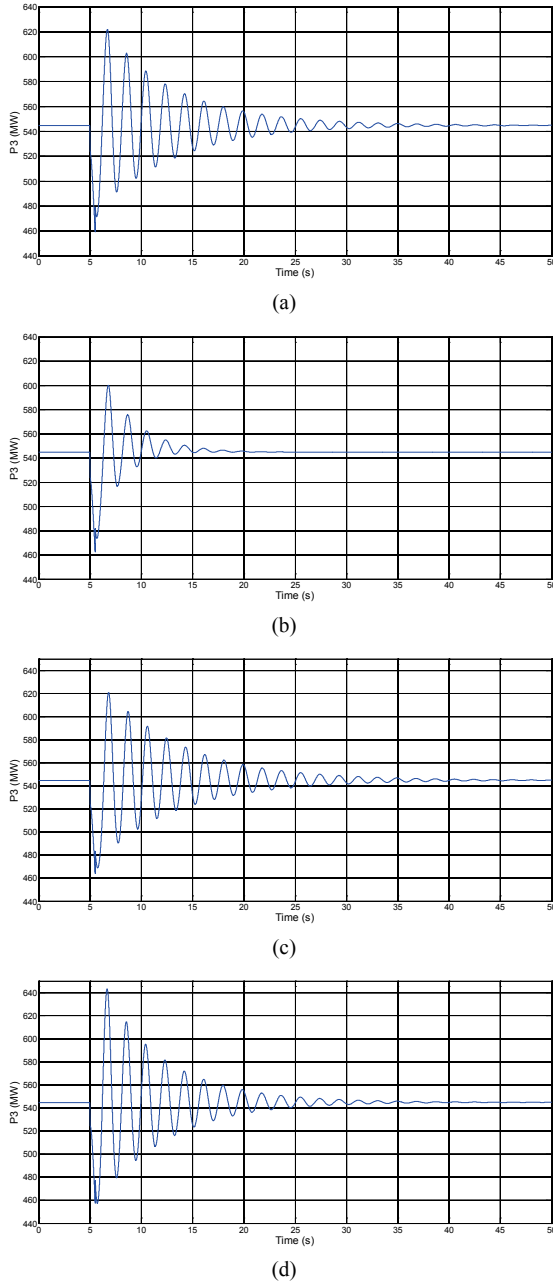


Fig.7. Active power generation from generator 3 under different damping conditions: (a) no damping controller; (b) input  $\Delta\omega_{r3}$  parameter PARA1; (c) input  $\Delta\omega_{r1}$  parameter PARA1; (D) input  $\Delta\omega_{r1}$  parameter PARA2

To validate the modal analysis results, time domain simulations with a load event at 5s are conducted under the four damping conditions and the active power generation from generator 3 is shown in Fig. 7

## VII. CONCLUSION

Based on the third-order model of the synchronous generator, this paper analyses the influence of SSSC on power system small signal stability in a single-machine infinite bus system. The block diagram representation of the system small signal performance could be extended for multi-machine system. The fundamental design method of SSSC damping controller is based on this block diagram. However, the zero-phase-shift design might face some problems in multi-machine system. By changing the phase shift, the designed SSSC damping controller can be adaptive to inputs from different generators in the connected system.

As the future work from this paper, the effects and coordination of multi-SSSC damping controllers within larger system will be studied. The coordination of SSSC damping controller and other types of power system oscillation damping controllers is another target.

## REFERENCES

- [1] K. Wang, Y. Q. Jin, D. Q. Gan, P. Ju, L. B. Shi and Y. X. Ni, "Survey of power system small signal stability and control," *Electric Power Automation Equipment*, vol. 29, no. 5, pp.10-19, May 2009.
- [2] F. J. Swift and H. F. Wang, "Application of the controllable series compensator in damping power system oscillations," *Proc. IEE-Generation Transmission Distribution*, vol. 143, no. 4, pp. 359-364, July 1996.
- [3] H. F. Wang, "Design of SSSC damping controller to improve power system oscillation stability," *Proc. IEEE AFRICON 1999*, vol. 1, pp. 495-500, September 1999.
- [4] B. S. Rigby and R. G. Harley, "An improved control scheme for a series-capacitive reactance compensator based on a voltage-source inverter," *IEEE Transactions on Industry Applications*, vol. 34, no. 2, pp. 355-363, March/April 1998.
- [5] B. S. Rigby, N. S. Chonco and R. G. Harley, "Analysis of a power oscillation damping scheme using a voltage-source inverter," *IEEE Transactions on Industry Applications*, vol. 38, no. 4, pp. 1105-1113, July/August 2002.
- [6] W. Qiao, R. G. Harley and G. K. Venayagamoorthy, "Effects of FACTS device on a power system which includes a large wind farm," *Proc. Power systems conference and exposition 2006*, pp. 2070-2076, November 2006.
- [7] W. Qiao and R. G. Harley, "Indirect adaptive external neuro-control for a series capacitive reactance compensator based on a voltage source PWM converter in damping power oscillations," *IEEE Transactions on Industrial Electronics*, vol. 54, no. 1, pp. 77-85, February 2007.
- [8] P. Kundur, *Power System Stability and Control*. New York: McGraw-Hill, 1994.
- [9] C. Su, Z. Chen, "An optimal power flow (OPF) method with improved power system stability," *IEEE International Universities Power Engineering Conference (UPEC)*, pp. 1-6, 2010.
- [10] K. K. Sen, "SSSC – Static synchronous series compensator: theory, modeling and applications," *IEEE Transactions on Power Delivery*, vol. 13, no. 1, pp. 241-246, January 1998.